

Numerical Simulation of gas-solid interfaces with large deformations

O.Y. Vorobiev and I.N. Lomov

This article was submitted to
International Conference on Computational Engineering Science,
Los Angeles, CA, August 21-25, 2000

February 1, 2000

U.S. Department of Energy

Lawrence
Livermore
National
Laboratory

DISCLAIMER

This document was prepared as an account of work sponsored by an agency of the United States Government. Neither the United States Government nor the University of California nor any of their employees, makes any warranty, express or implied, or assumes any legal liability or responsibility for the accuracy, completeness, or usefulness of any information, apparatus, product, or process disclosed, or represents that its use would not infringe privately owned rights. Reference herein to any specific commercial product, process, or service by trade name, trademark, manufacturer, or otherwise, does not necessarily constitute or imply its endorsement, recommendation, or favoring by the United States Government or the University of California. The views and opinions of authors expressed herein do not necessarily state or reflect those of the United States Government or the University of California, and shall not be used for advertising or product endorsement purposes.

This is a preprint of a paper intended for publication in a journal or proceedings. Since changes may be made before publication, this preprint is made available with the understanding that it will not be cited or reproduced without the permission of the author.

This report has been reproduced
directly from the best available copy.

Available to DOE and DOE contractors from the
Office of Scientific and Technical Information
P.O. Box 62, Oak Ridge, TN 37831
Prices available from (423) 576-8401
<http://apollo.osti.gov/bridge/>

Available to the public from the
National Technical Information Service
U.S. Department of Commerce
5285 Port Royal Rd.,
Springfield, VA 22161
<http://www.ntis.gov/>

OR

Lawrence Livermore National Laboratory
Technical Information Department's Digital Library
<http://www.llnl.gov/tid/Library.html>

Numerical Simulation of gas-solid interfaces with large deformations

O.Yu Vorobiev, I.N Lomov
Geophysics and Global Security Division
P.O Box 808, L-206, LLNL, CA 94550
e-mail: oleg@s90.es.llnl.gov

Summary

A method of treatment of multimaterial interfaces on Eulerian grids is developed which works well for mixtures of materials with diverse compressibilities and shear moduli. This makes it possible to use this method not only for problems of gas dynamics and solid mechanics but also to model fluid-structure interaction problems.

Introduction

Accurate treatment of gas-solid interfaces is very important for variety of problems including fluid-structure interactions. Using Lagrangian grid offers the most natural way of modeling of moving multimaterial interfaces. Unfortunately this approach experiences difficulty in the problems with large material deformations because of mesh tangling and crashes. The time step controlled by strongly deformed mesh cells due to stability limit drops down and makes calculations inefficient. To continue calculations mesh remapping is required which makes algorithm more complex and time consuming.

In Eulerian codes the grid cells may contain several materials with dramatic difference in shock impedance (for example, gas-solid interface). When waves pass through such cells they may cause over-compression or expansion of materials with high shock impedance if the same velocity is used for all flow components in the cell. Instead of introducing different velocities for each component we are trying to solve solid-gas problems by distributing total deformations among components according to their compressibilities and shear modulas.

1. The system of equations of motion

The volume fraction, mass, momentum and energy conservation laws for a mixture of N materials can be expressed in invariant form as following:

$$\begin{aligned}\frac{\partial f_\alpha}{\partial t} + \nabla \cdot (f_\alpha \mathbf{v}) &= f_\alpha \frac{K}{K_\alpha} \nabla \cdot \mathbf{v}, \quad \alpha = 1, N; \\ \frac{\partial \rho_\alpha f_\alpha}{\partial t} + \nabla \cdot (\rho_\alpha \mathbf{v} f_\alpha) &= 0, \quad \alpha = 1, N; \\ \frac{\partial \rho \mathbf{v}}{\partial t} + \text{div}(\rho \mathbf{v} \otimes \mathbf{v} - \mathbf{T}) &= \rho \mathbf{q}; \\ \frac{\partial \rho_\alpha f_\alpha \varepsilon_\alpha}{\partial t} + \nabla \cdot (\rho_\alpha \varepsilon_\alpha f_\alpha \mathbf{v}) - \nabla \cdot (\mathbf{T} \mathbf{v} \eta_\alpha) &= \rho_\alpha f_\alpha (\mathbf{q} \cdot \mathbf{v} + w_\alpha), \quad \alpha = 1, N;\end{aligned}\tag{1}$$

Where f_α , ρ_α - and $\varepsilon_\alpha = E_\alpha + \frac{1}{2}v^2$ are the volume fraction, density and the total specific energy of the component α , \mathbf{v} - is the average mass velocity, \mathbf{T} -is the average stress tensor. The right side of the eq(1.1) accounts for compressibility of the flow, so that the changes in the volume of each material is proportional to $1/K_\alpha$ and cause roughly the same pressure change. The terms \mathbf{q} and w in the right side of (1) are the bulk forces and energy sources correspondently. By summing Eq.(1.2) and Eq.(1.4) we get total mass and energy conservations for the mixture, since $\sum_\alpha f_\alpha = 1$, and $\sum_\alpha \eta_\alpha = 1$. Parameter η_α (the third term in Eq.1.4) is a fraction of PdV work done with material α during the deformation to be determined below. One way of partition of PdV term for multifluid flow was suggested in [1], where it was represented in nonconservative form as $\frac{f_\alpha K}{K_\alpha} P \nabla \cdot \mathbf{v} + \frac{f_\alpha \rho_\alpha}{\rho} \mathbf{v} \cdot \nabla P$ (2)

The derivation of Eq.(2) was based on the pressure equilibrium among components. We have found that using (2) leads to an excessive heating and acceleration of a gas adjacent to a solid when the shock wave emerges from the solid. This is because in the numerical approximation the assumption of instantenious pressure equilibrium is not valid, since it takes a few time steps for the pressure wave to cross a grid cell from stability condition and materials may have deviatoric stresses and, consequently may have different pressure even after the passage of the wave. Assuming that PdV contribution for component α is proportional to $P_\alpha dV_\alpha \sim P_\alpha / K_\alpha$ we get $\eta_\alpha = \frac{f_\alpha K P_\alpha}{K_\alpha P}$ (3)

Assuming $P_\alpha \sim K_\alpha$ we get more simple formula, which gives distribution of PdV work proportional to masses as $\eta_\alpha = f_\alpha \rho_\alpha / \rho$ (4)

The average stress tensor is calculated as $\mathbf{T} = -K \sum_\alpha \frac{P_\alpha f_\alpha}{K_\alpha} \mathbf{I} + G \sum_\alpha \frac{\mathbf{T}'_\alpha f_\alpha}{G_\alpha}$; (5)

where the first term in (5) represents the average pressure and the second one represents deviatoric stress. The average bulk and shear moduli are calculated as

$$K = \left(\sum_\alpha \frac{f_\alpha}{K_\alpha} \right)^{-1}; G = \left(\sum_\alpha \frac{f_\alpha}{G_\alpha} \right)^{-1} \quad (6)$$

If the elastic deformation tensor \mathbf{B}_α is known, the deviatoric stress can be calculated for every component as

$$\mathbf{T}'_\alpha = G_\alpha (1 - \Phi_\alpha) \mathbf{B}'_\alpha \rho_\alpha / \rho_{0\alpha} \quad (7)$$

where G is the shear modulus, Φ_α is the reference porosity, ρ_α and $\rho_{0\alpha}$ are respectively the current and the reference density for material α .

To describe elastic-plastic behavior, we use the following equation for the unimodular tensor of elastic distortional deformation \mathbf{B}_α [2].

$$\dot{\mathbf{B}}_\alpha = \mathbf{L}_\alpha \mathbf{B}_\alpha + \mathbf{B}_\alpha \mathbf{L}_\alpha^T - \frac{2}{3} (\mathbf{D}_\alpha \cdot \mathbf{I}) \mathbf{B}_\alpha - \Gamma_p^\alpha \left[\mathbf{B}_\alpha - \frac{3\mathbf{I}}{\mathbf{B}_\alpha^{-1} \cdot \mathbf{I}} \right]; \quad (8)$$

Γ specifies the plastic response of the material and is taken to be a function of the von Mises effective stress and the yield strength. For rate-dependent response, we used the function proposed by Swegle and Grady [3].

In (8) \mathbf{L} - is the velocity gradient tensor, \mathbf{D} - is it's symmemtric part. Although we use the same velocity \mathbf{v} for all components, the effective velocity gradient acting in each material differs from the average velocity

ICES2K Conference, August 2000, Los Angeles, USA

gradient \mathbf{L} calculated for the mixture on the basis of the velocity field. We use the following formula for L_α

which gives a volume conservation $\left(\sum_{\alpha} \mathbf{D}_{\alpha} \cdot \mathbf{I} = \mathbf{D} \cdot \mathbf{I} \right)$

$$L_{\alpha} = \mathbf{L} \frac{Gf_{\alpha}}{G_{\alpha}} \quad (9)$$

2. Numerical Integration

Since eqs.(1) are written in conservative form they can be integrated numerically on a fixed or moving grid using Godunov's method. In the present work rectangular grid is used and all flow parameters are cell centered. To calculate fluxes the normal velocities $V_{1,2,3,4}^n$, the tangential velocities $V_{1,2,3,4}^t$ and corresponding stresses are to be known at cell interfaces. To find these parameters linearized Riemann problem for perfectly elastic material is solved. Because of each cell may contain several materials including vacuum, averaged cell parameters are used in Riemann solver. In multifluid cells the multimaterial interface is reconstructed using VOF approach similar to [4]. When both the interface orientation and the normal mass velocities $V_{1,2,3,4}^n$ are known the amount of each material flowing into or out of the cell can be found. When solving linearized Riemann problem we neglect the curvature of isentropes and replace them in each point by a straight line (see, for example, points **C**, **B** in Fig.1) Our experience shows that using such linearized Riemann solver gives very closed results to ones obtained with the exact Riemann solver if the pressure is of the order of $\rho_0 c_0^2$ or less. For solids this pressure is about 1 Mbar, what is two orders of magnitude high than the material strength. For gases the change of the sound velocity (which gives the curvature of isentropes) can be dramatic on the same pressure scale and more accurate approximate Riemann solvers are needed (for example, [5,6]). Special care is also required for metastable states realized in two-phase region. Using locally linear approximation of isentropes can give negative density or unphysically high mass velocity due to the sound velocity drop in two-phase region (see, for example, point A in Fig. where approximated isentrop AD gives negative density). To fix this we replace release isentropes in such points by the straight line (see OA in Fig.1) connecting zero density zero pressure point with the given point any time the density in rarefaction becomes negative during one increment.

The velocity gradient tensor \mathbf{L} is approximated by (10) using normal and tangential velocities found at the cell interfaces after solving the Riemann problem (see Fig.2)

$$L_{11} = \frac{V_2^n - V_1^n}{\Delta_{12}}; L_{22} = \frac{V_4^n - V_3^n}{\Delta_{34}}; L_{12} = \frac{V_4^t - V_3^t}{\Delta_{34}}; L_{21} = \frac{V_2^t - V_1^t}{\Delta_{12}}; \quad (10)$$

We split equations (1) into two different sets of equations corresponding to X and Y directions. The integration of the whole system of equations includes 3 steps:

- I. The sweep in X (or Y) direction
- II. The sweep in the other direction
- III. Update of the elastic distortion tensor \mathbf{B}_{α} for each component by solving eq.(8) after the velocity gradient tensor \mathbf{L} has been approximated in two previous steps.

For the purpose of numerical stability the direction of the first sweep changes from one time step to the other.

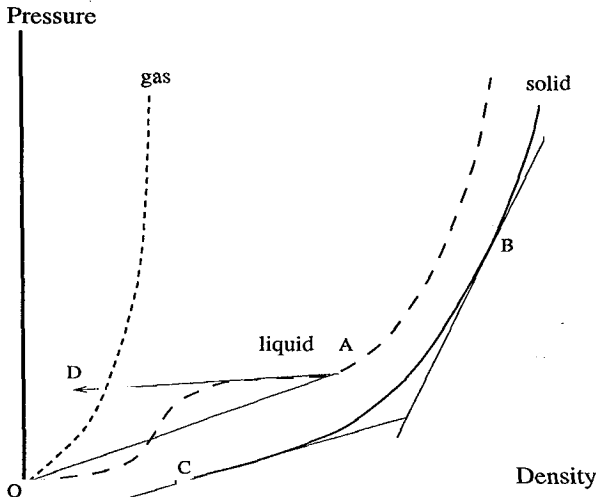


Fig.1 Schematic view of isentropes for different states of matter in density-pressure coordinate plane

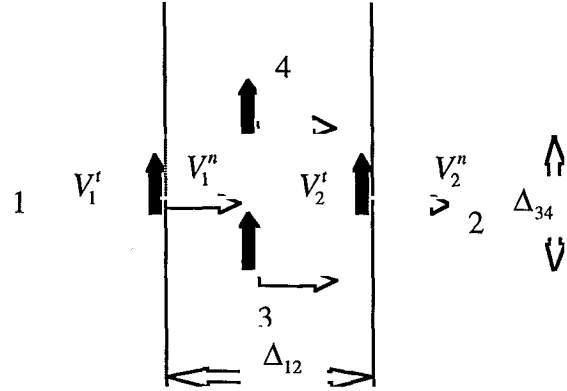
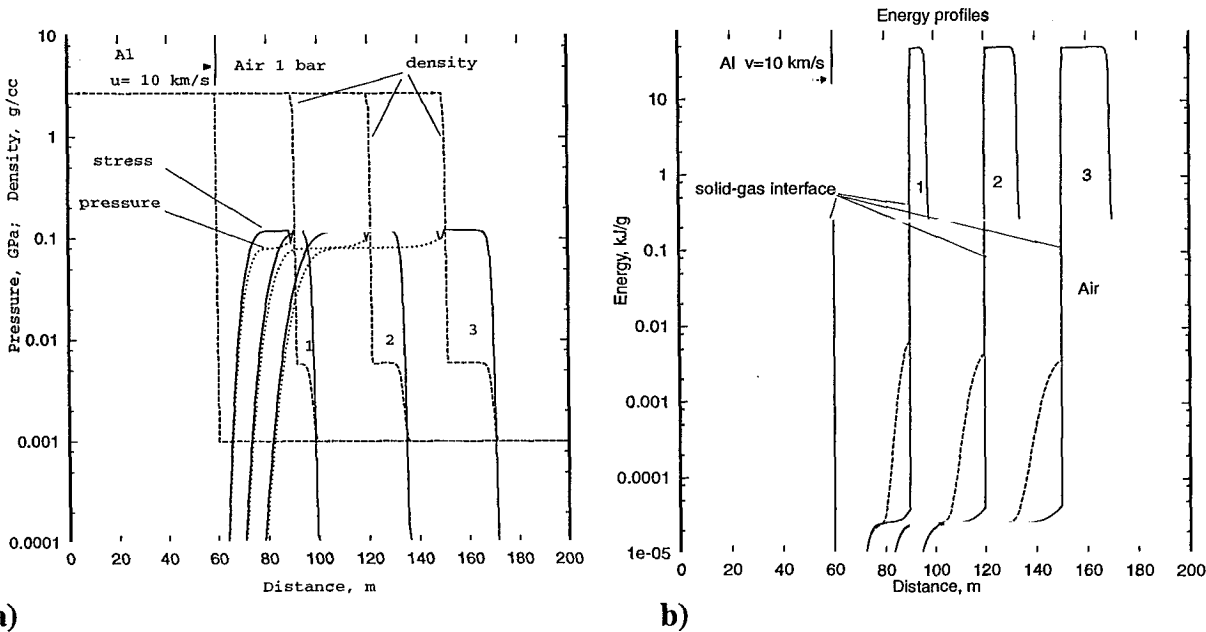


Fig.2 Scheme of velocity gradient tensor calculation. The black and white arrow show the tangential and normal velocities found at the cell interfaces by solving Riemann problem.

Demonstrative Calculations

The simplest test for gas-solid interface treatment is a plane 1D impact of solid onto gas. If the impact velocity is high, the shock wave moving into gas can be considered as a strong one and the density behind the shock should approach $\frac{\gamma+1}{\gamma-1}$ of the initial gas density. Results of 10 km/s impact of aluminum layer onto air at 1 bar is shown in Fig.3. The stress is constant across the interface but the pressure is different due to the presence of deviatoric stresses in aluminum. We found that the equal distribution of specific internal energy increment due to Lagrangian work in multifluid cells (Eq.(4)) gives almost as good results as when



a)

b)

Fig.3. The pressure (dotted lines), stress, density profiles a) and b) the specific internal energy profiles for plane impact of aluminum (on the left) on air (on the right). The impact velocity is 10 km/s. The time moments are 1- 3 ms, 2- 6ms, 3-9ms.

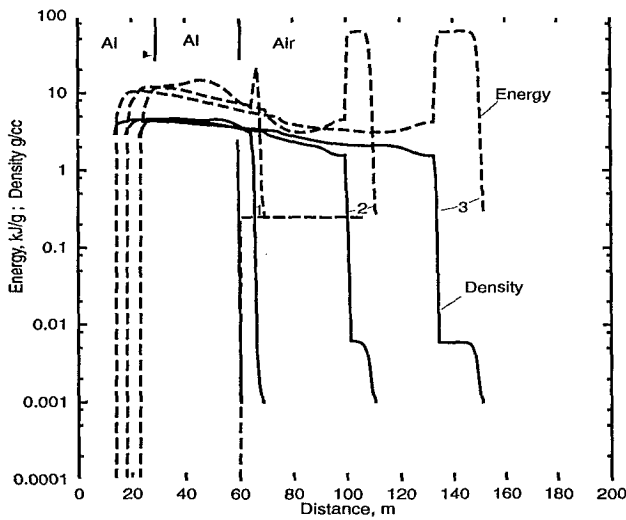


Fig.4. The energy and density profiles for a shock wave emerging from the solid into air at 1 bar. The mass velocity behind the shock is 5 km/s. The time moments are: 1-3 ms, 2-6ms, 3- 9ms.

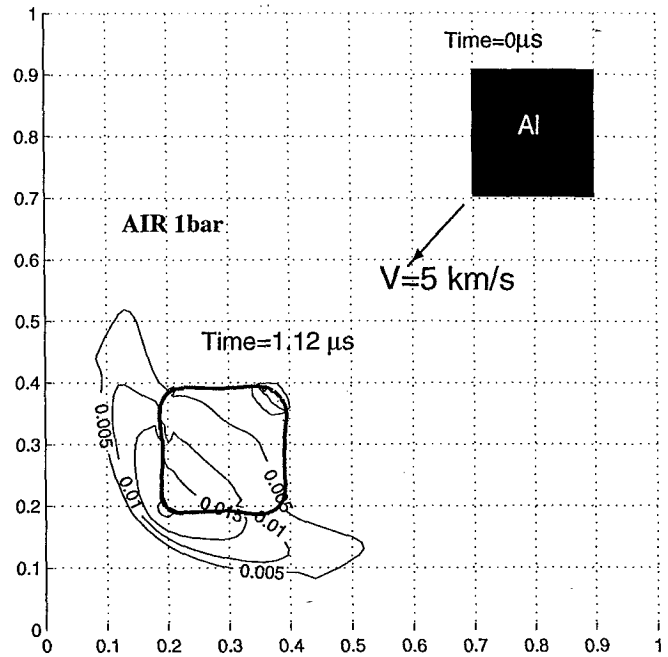


Fig.5. 2D translation test: aluminum moving in the air

Eq.(3) is used. The difference can be found in energy profiles (see Fig.3.b), where simulation results obtained using Eq.(4) are shown with dashed lines. Using Eq.(4) leads to overheating of the metal impacting air. However, this artificial heating is one order of magnitude smaller than the melting energy even at 10 km/s impact velocity.

The second test is a shock wave coming from a solid into a gas. The energy and density profiles for this test are shown in Fig.4.

Fig.5. demonstrates 2D simulation results of aluminum bar moving through the air in the diagonal direction with 5 km/s. The lines of constant pressure and the material interface are shown in low left corner for the time 1.12 μ s. This test represents the most general 2D case when the velocity of the solid object is not aligned with the grid lines.

Conclusions

We have demonstrated an effective method to introduce strength models into Godunov type hydrocodes. Since high order Godunov methods are widely used in computational fluid dynamics due to their superiority in treatment of flows with strong shocks and discontinuities, the present method extends these benefits to include problems of solid mechanics and fluid-structure dynamics in the case of large deformations. The method can be generalized to 3D by introducing an appropriate interface reconstruction algorithm.

References

1. Miller, G.H.; Puckett, E.G., (1996), "A high-order Godunov method for multiple condensed phases", Journal of Computational Physics, 128, (no.1):134-64.
2. Rubin, M., Vorobiev, O., Glenn, L. Mechanical and Numerical Modeling of a Porous Elastic-Viscoplastic Material with Tensile Failure, to be published in International Journal of Solids and Structures 1998

ICES2K Conference, August 2000, Los Angeles, USA

3. Swegle, J. W. and Grady, D. E., (1986), "Shock Viscosity And the calculation Of Steady Shock Wave Profiles", in Shock Waves In Condensed Matter, edited by Y. M. Gupta (Plenum, New York), 353-357.
4. Youngs, D.L., (1982), "Time-dependent multi-material flow with large fluid distortion", in K.W.Morton and M.J.Baines (eds), Numerical Methods for Fluid dynamics, Academic, New York, 273-285
5. Colella, P., Glaz, H.M., (1985), "Efficient solution algorithms for the Riemann problem in real gases", J.Comput.Phys., 58, 264
6. Dukowicz, J., (1985) A General, Non-Iterative Riemann Solver for Godunov's Method, J.Comput.Phys., 61, 119

This work was performed under the auspices of the U. S. Department of Energy by the University of California, Lawrence Livermore National Laboratory under Contract No. W-7405-Eng-48.